

# Wire-bonds failures Induced by resonant vibrations in the CDF silicon detector

G. Bolla<sup>1,\*</sup>, M. Atac<sup>2</sup>, V. Pavlicek<sup>2</sup>, G. Cancelo<sup>2</sup>, S. Nahn<sup>3</sup>, R. Mumford<sup>4</sup>, M. Garcia-Sciveres<sup>5</sup>, T. Nguyen<sup>2</sup>, S. Forrester<sup>6</sup>, C. Hill<sup>7</sup>, J. Olszewski<sup>1,2</sup>, A. Rahaman<sup>8</sup>, J. Goldstein<sup>9</sup>, B. Ashmanskas<sup>10</sup>, T. Maruyama<sup>11</sup>, R. S. Lu<sup>12</sup>, J. Spalding<sup>2</sup>, Z. Tang<sup>2</sup>, T. Zimmerman<sup>2</sup>, S. Moccia<sup>2</sup>, J. D. Lewis<sup>2</sup>

**Abstract**--Unrecoverable internal failures of modules in the CDF Run2 silicon detector have been observed since its installation in early 2001. A fraction of these failures have been categorized as infant mortality because they were detected right after installation or in the first few months of data taking. Another fraction occurred during the second year of operation and they were strongly correlated with anomalous trigger conditions. These failures are explained by wire-bonds breaking due to fatigue stress induced by resonant vibration. These resonant vibrations are a direct consequence of the oscillating Lorentz forces induced by the 1.4 T magnetic field on wire-bonds carrying non-DC current. Changes have been implemented in data taking procedures in order to minimize occurrences of such failures and to prolong the lifetime of the detector itself. A more general analysis of the topic has been pursued. Changes in the packaging and assembly processes for future applications have been investigated and are proposed in order to avoid this failure mode.

## I. INTRODUCTION

CDF is a collider experiment that is running at the Tevatron. The core of the CDF detector is an 8 layer silicon micro strip tracker. There are over 722K active strips with pitches that range from 25 to 140  $\mu$ m. Wire-bonds are widely used for signals, commands and power connections between the various components of the modules. Long after the end of the detector commissioning phase a non-negligible rate of permanent failures (14 failures in 704 modules) was recorded. A strong time correlation between the occurrences of the failures and anomalous trigger conditions was promptly noted. An investigation started in order to understand these trigger dependent failure modes and possibly reduce or remove their rate of occurrence. The silicon detector was installed in the CDF experiment in January 2001. A general description of the system can be found elsewhere [1]. A schematic view of the CDF silicon is shown in fig.1. Once installed it is not accessible for maintenance and a direct investigation on the

faulty modules is not possible. The investigation had to be pursued with spare parts left over after construction [2]. The emulation on the bench of the anomalous trigger conditions was not sufficient to reproduce the failure modes until the modules were placed in a 1.4 T magnetic field. Oscillating Lorentz forces on the wire-bonds induced by non-DC currents were found to excite resonance movements of the *Al* wires. During this motion fatigue stress is accumulated at the wire-bond heel until the wire breaks and the electrical connection is lost.

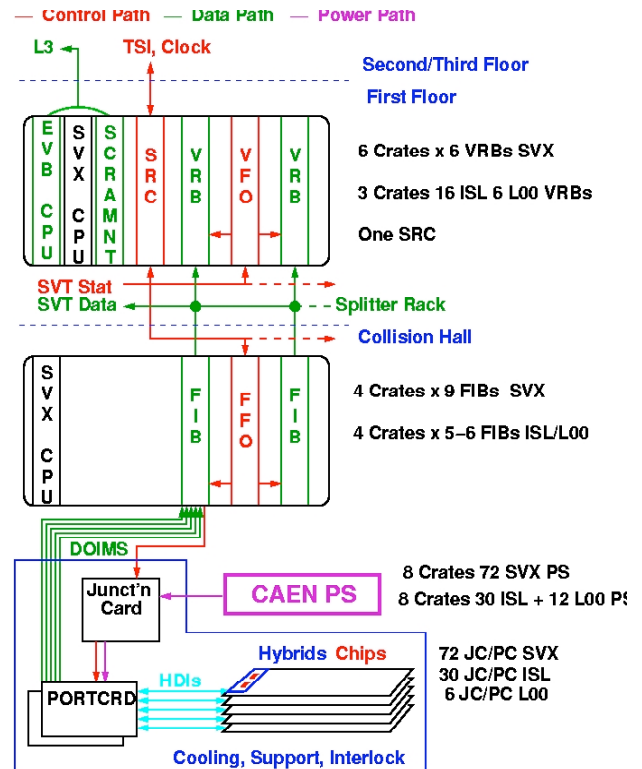


Fig. 1. Schematic view of the CDF silicon system. To be noticed that all of the components in the blue box in the bottom of the figure are not accessible after the installation in the CDF experiment. Wire-bonds are widely used on the portcard and on the hybrids for electrical interconnections.

This paper presents the symptoms associated with the failure modes, a comprehensive description of the current consumption on the power lines that failed and the consequent Lorentz forces on the wire-bonds. Furthermore, a qualitative and quantitative analysis of the general behavior of wire-bonds

<sup>1</sup> Purdue University, W. Lafayette, IN 47907 USA  
<sup>\*</sup> Contact informations: PO Box 500 Fermilab, MS 223 CDF, Batavia IL 60510. bolla@fnal.gov.  
<sup>2</sup> Fermi National Accelerator Laboratory, Batavia, IL 60510 USA  
<sup>3</sup> Yale University, New Haven, Connecticut, 06520 USA  
<sup>4</sup> Johns Hopkins University, Baltimore, Maryland 21218 USA  
<sup>5</sup> Lawrence Berkeley Laboratory, Berkeley, CA 94720 USA  
<sup>6</sup> University of California, Davis, CA 95616 USA  
<sup>7</sup> University of California, Santa Barbara, CA 93106 USA  
<sup>8</sup> University of Pittsburg, Pittsburg, PE 15260 USA  
<sup>9</sup> CCLRC Rutherford Appleton Laboratory, Chilton Didcot Oxford, UK  
<sup>10</sup> Argonne National Laboratory, Argonne, IL 60439 USA  
<sup>11</sup> University of Chicago, Chicago, IL 60637 USA  
<sup>12</sup> Academia Sinica, Taipei, Taiwan, 11529, Republic of China

in a magnetic field with non-DC current in the 1-50 KHz range is described.

## II. DESCRIPTION OF THE FAILURES

The command and data flow within the CDF silicon system is described in fig.1. Commands are generated in the VME crates and routed to the tracking volume. Here they are received by the portcard [3] and fanned out to 5 ladders (single independent readout unit in the system) where the SVX3d [6][7] read-out chips integrate the charge, digitize it and send the data out through a 8 bits parallel bus. The data are then sent from the portcard to the VME through a parallel optical link from now on called DOIM (Dense Optical Interface Module)[5]. For the failure mode described here the possibility of the *A* wire fusing due to excess current has been ruled out by introducing a short-circuit (and so maximum current draw) and verifying that the tripping mechanism of the power supplies always reacts before any permanent damage occurred in the wires. Possible aging effects (e.g. electron migration) inducing the loss of electrical continuity were ruled out by accelerated aging tests performed at high temperature with spare parts.

The CDF detector is designed to run with a level 1 trigger (L1A) rate up to 50 KHz. At each one of these triggers the silicon system is read out and its data are used in the second trigger level to select events with displaced tracks. All the failures described here appeared during trigger conditions where the L1A were issued according to well defined synchronous conditions. The distribution of the time interval between L1A in the experiment is usually very broad due to the natural randomness of the physics processes being investigated. During specific tests trigger were issued according to the repetitive beam structure so the silicon system was read out with fixed intervals between a L1A and the next one. These conditions were induced to explore the maximum sustainable rates for the experiment.

The failures experienced in the CDF silicon detector can be grouped into two categories, affecting two pieces of the detector, the jumper and the DOIMs. Both groups share the time behavior of the current consumption and its correlation with the trigger rates of the experiment.

### A. The DVDD jumper failure

The Double-Sided silicon Detectors (DSSD) in the SVXII modules [3] are readout by a daisy chain of SVX3d chips. The connections between the Phi and the Z hybrid for commands, power and data is established by a ceramic substrate (jumper) with pass-through via holes that is glued on the sensor's edge and wire-bonded to both hybrids. The jumper provides electrical continuity from one side to the other. A simple schematic of this interconnection is shown in fig.2. Both the analog (AVDD) and digital (DVDD) power lines as well as their return ground paths are connected with two redundant wire-bonds while single wires are used for the commands and data lines.

Twelve of the fourteen failures described in this paper share the same symptoms:

- Lack of data from the Z chips
- Decrease in the DVDD power consumption

- Increase on the AVDD power consumption

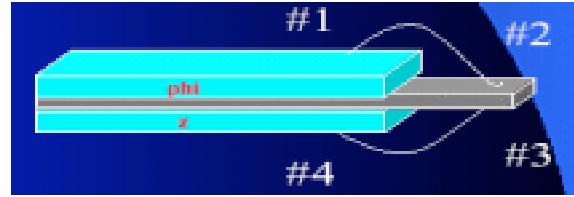


Fig.2. Simple schematic of the jumper connection via wire-bonds.

The symptoms have been successfully reproduced without any ambiguity on the bench with spare modules by pulling the DVDD jumper wire-bonds. The digital power consumption of the chips is strongly dependent on the activities of its digital part. Fig.3 shows the current behavior through the DVDD jumper connection during a DIGITIZE-READOUT sequence that is triggered by a CDF L1A (the jumper wire-bonds were replaced by a discrete wire in order to use a Tektronix A6302 current probe). It can be noticed how the current quickly changes by more than 100 mA within a few micro seconds while the readout switches from the Phi to the Z side of the module. The amount of time spent in the high current state is directly proportional to the occupancy on the Z side.

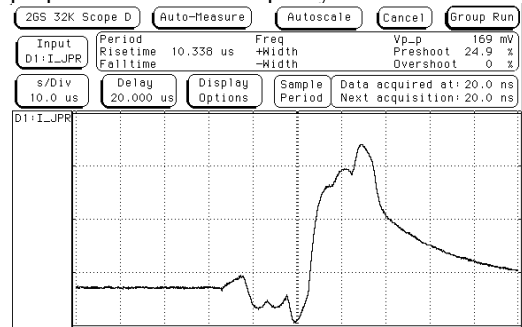


Fig.3 Current through the DVDD jumper connection (Digital power supply) versus the time during L1A-DIGITIZE-READOUT sequence (this plot is for a six chip ladder). Each division is 10 ns on the X-axis and 50 mA in the Y-axis. At about 33 ns from the left border the SVX3 chips start the digitization. The current linearly increase for about 5 ns. At the end of the digitization the Phi chips are readout first. In the center of the graph we have the transition when the Phi chips read-out is completed and the Z chips start to send out the data. The current through the DVDD jumper connection rises by 100-150 mA. A plateau is reached within a few ns. As long as there are data on the chips to be readout the current stays at this value until read out is completed and then slowly goes back to the steady state value.

### B. The DOIM failure

The data from the SVX3d chips are received on the portcard where the DOIMs (one per module so five per portcard) send them to the VME buffers. Two of the 14 failures described in this paper share the same symptoms:

- Lack of data from the whole module
- Decrease by 1/5 of the DOIM power consumption within the portcard.

Once again the symptoms have been successfully reproduced on the bench with spare parts by pulling the power wire-bonds between the portcard and the DOIM.. The power consumption of a single DOIM is about 350 mA. The current amplifiers drive either the laser diodes (for bit HIGH) or a dummy resistive load (for bit LOW). The matching of the two loads is not perfect and therefore implies current pulses of a few mA

between idle state and during data transmission. Out of 18 spare packages that were tested the maximum current variation detected was 7 mA. The limited number of tested parts cannot rule out larger variation on some of the 504 installed in the CDF system. The current variation is not always in the same direction. Direct measurements of the current swing on those installed in CDF are not reliable due to the fact that the same power supply (and therefore the same ammeter) feed five on a portcard.

### III. LORENTZ FORCES AND RESONANT BEHAVIOR

The geometry of the DVDD jumper bond is shown in fig.4 as measured with a coordinate measurement machine at the Silicon Detector Facility at Fermilab. The magnetic field is directed orthogonal to the plane of the wire as if entering the plane of the paper. As a consequence the  $AI$  wire is exposed to a distributed force while current is flowing through it. In CDF the magnetic field is 1.4 T, which together with a current of 200 mA results in a Lorentz force of 28 milligrams per millimeter of wire length. This is a couple of orders of magnitude smaller than what is required to pull a healthy wire-bond to failure. The movement induced in the wires from these forces has been estimated to be on the order of a few micrometers and therefore hard to detect with optical tools.

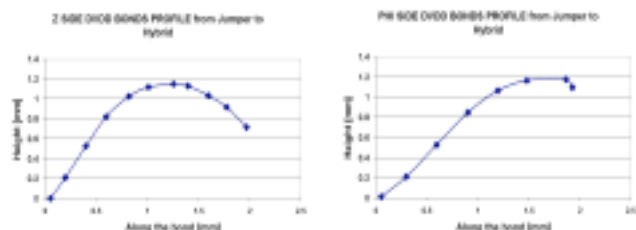


Fig.4 Geometry of the DVDD jumper bonds Z and Phi side from left to right. On each picture X=0 correspond to the bond foot on the jumper.

A Finite Element Analysis (FEA) of the system resulted in the natural resonant frequencies listed in TABLE I. In fig.5 a graphical view of the natural modes of the oscillation is shown with the relative resonant frequencies as simulated for a bond with the same shape as the Phi side DVDD jumper connection. Further details on the results of the FEA can be found in [8]. The first three natural resonant modes of the wires are well inside the operational range of the experiment.

TABLE I  
CALCULATED RESONANCE FREQUENCIES

Bond type	Frequency [KHz]	Plane of motion w.r.t. the plane of the wire
Z	14.2	Perpendicular
Z	37.2	Coplanar
Z	42.0	Perpendicular
Z	83.0	Coplanar
Z	84.7	Perpendicular
Phi	20.4	Perpendicular
Phi	39.8	Coplanar
Phi	55.2	Perpendicular
Phi	103.6	Coplanar
Phi	111.5	Perpendicular

First 5 Frequencies and Modes of the  $\phi$ -side Bonds

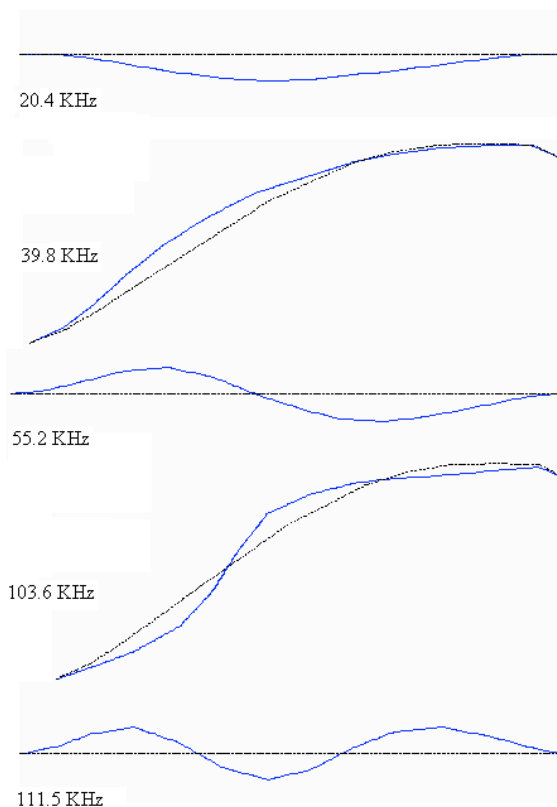


Fig.5 Graphical view of the oscillating modes for the Phi side DVDD jumper wire-bond geometry. The black lines (straighter) represent the shape of the bond at rest while the blue lines show its position during oscillations.

Small test boards with wire-bonds of similar geometry as the ones of fig.4 were built to verify the results of the FEA. A pulse generator and a current amplifier were used to deliver current sine waves or current pulses through the wires. The current and the frequencies were tunable with 1 mA and 10 Hz precision respectively. Magnifying optics and a 40,500 frames per second fast video equipment were used to monitor the motion of the  $AI$  wires. The FNAL Technical Division calibration magnet was used to generate the 1.4 T magnetic field. The orientation of the bonds with respect to the magnetic field was the same as for the CDF silicon modules. Frequency scans were performed with sine waves of 100 mA amplitude. Resonant behavior was detected at frequencies close to the ones predicted by the FEA at 14 and 26 KHz. The discrepancy can be attributed to a slightly different shape of the bonds under test with respect to the ones simulated. In the case of current pulses a resonant frequency  $f$  could be excited with a train of pulses at frequency  $f, f/2, f/4$  etc. A full frequency scan up to 50 KHz was difficult to perform on each bond. The wires break at the heel in time scale of minutes, corresponding to  $10^5$ - $10^6$  cycles, that is comparable to the time to perform the scans. In fig.6 the broken surface of a pulled bond foot is compared to one of a bond foot that broke due to

fatigue stress accumulated at the heel. These pictures are in good agreement with previous work [10].

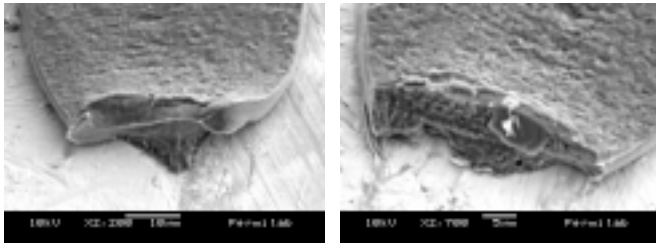


Fig.6 SEM picture of broken bond heels. On the left the pure ductile surface of a bond heel that has been broken with the usual pull-test is shown while the one on the right broke due to fatigue stress induced by the resonant vibrations and shows a brittle surface.

The motion of the wires was recorded in short movies with the fast video camera. The images were digitized on a frame-by-frame basis. The position of the wire versus frame number was plotted in ten bin intervals and a sinusoidal fit gave the amplitude of the motion. A wire-bond was fed with a train of 40 current pulses with a period of 108  $\mu$ sec, a duty cycle of 12 % and amplitude of 70 mA. In fig.7 the amplitude of the motion versus frame number is plotted. During the first 20 frames no pulses are released. At frame 20 the wave function generator is triggered to start the train. Only 3-4 pulses are necessary to start the motion of the wire. The amplitude of the motion grows linearly until frame 200 when the last pulse is delivered. The amplitude of the motion saturates at several wire diameters after 50-80 pulses depending on the driving force (pulse amplitude and width). The free exponential decay of the motion was used to calculate a dumping ratio of  $0.0076 \pm 0.0004$ . This value is very similar to the 0.01 used during the finite element analysis.

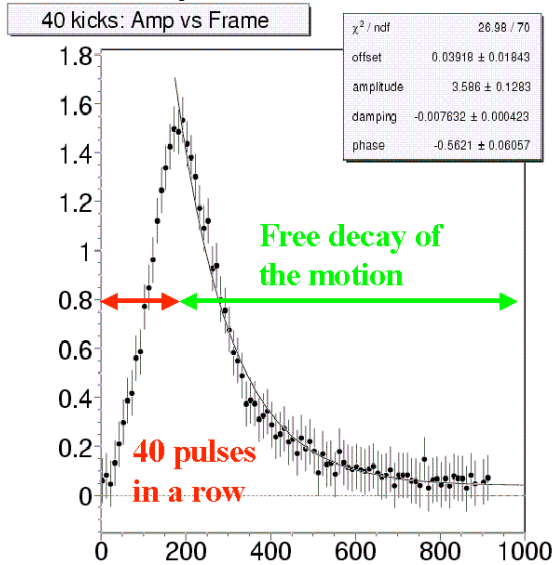


Fig.7 Amplitude of the motion versus frame number when a train of 40 current pulses is sent to the wire as described in the text.

The DOIM wire-bonds lie on a plane that contains the magnetic field. Due to the different height of the two substrates (there is a step up of  $\sim 300$  micrometers between the portcard and the DOIM bonding pads) and the loop height there is still a component of the wire that is orthogonal to the

magnetic field. Even in this case Lorentz forces can excite resonant vibrations. Furthermore the forces are now moving the wires from side to side. With this configuration we expect the amplitude of the motion to be larger than in the case of the DVDD jumper bonds. In fig.8 the amplitude of the motion versus the frequency of the pulses is plotted for the same wire-bond. The filled squares are measurements taken with the jumper orientation and the current pulses as previously described in this section, while the empty squares are measurements taken after rotating the wire under test by 90 degrees in order to emulate the DOIM orientation.

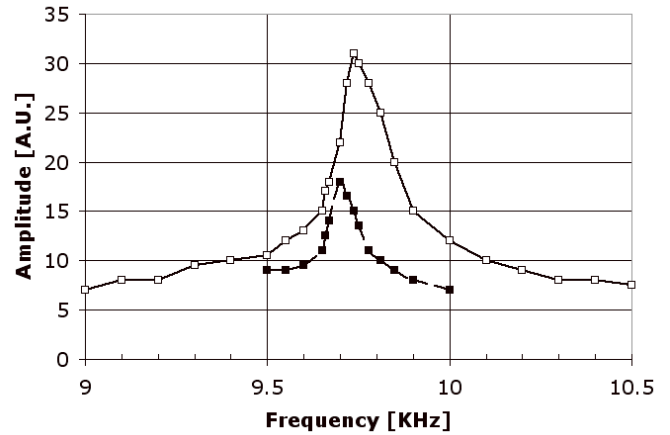


Fig.8 Amplitude of the motion versus frequency of the current pulses. Filled squares are for the jumper orientation while empty squares are for the DOIM orientation. The lines are joining the measured values and are there to guide the eye. The characteristics of the current pulses are described in the text.

For this second set of measurements the amplitude of the current pulses was diminished from 70 to 14 mA. With the current lowered by a factor of five the amplitude of the oscillation at its peak frequency is still a factor of two bigger than what is measured with the jumper orientation. This explains how the DOIM wires can break in the same way as the jumper wires even if pulsed with much smaller current amplitudes.

Four SVXII spare modules were placed in a second test magnet with a larger bore [9] in order to physically accommodate the 30 cm long devices. The synchronous trigger conditions were emulated in a 1.4 T magnetic field by forcing the DAQ into a fixed frequency mode of operations. This setup did not allow any optical monitoring of the motion of the wires. The symptoms associated with the failures previously described were the only available feedback. A slow and time-consuming frequency scan was necessary to reproduce the first failure. The DVDD jumper wire-bonds broke at their heel on the Phi bonds at a L1A frequency of  $\sim 10$  KHz. The frequency of the failure does not match any listed on table I but it is consistent with \_ of the first mode and \_ of the second one. The location of the breakage is consistent with the position of maximum stress as seen in the FEA.

Wire-bond encapsulation can prevent this failure mode. Different Coefficients of Thermal Expansion (CTE) of the various substrates used for these applications could also induce fractures on encapsulated bonds. For future applications this was addressed by depositing a silicon elastomer (Sylgard 186

silicon Elastomer from Dow Corning) only at the feet of the bonds. Due to surface tension the encapsulant adheres to the Al wire surface up to a height of 50-100  $\mu$ m. These wire-bonds were tested with the same procedures as described above. The amplitude of the vibration was measured to be more than one order of magnitude smaller than without the encapsulant. The bonds were pulsed for hours with 0.5 A pulses at resonant frequencies without any failure.

#### IV. OPERATIONAL RESPONSE IN THE EXPERIMENT

360 SVXII jumpers are used in the SVXII detector. Their wire-bonds are very similar in shape to the ones in fig.4 but cover a broad distribution due to variations during the construction process. Similar considerations apply to the 504 DOIM that are used. In order to mitigate the occurrence of the failures described above the current consumption on the affected power lines has been minimized by reducing the current output of the bus drivers on the SVX3d chips (this is a remotely programmable setting). The readout thresholds have been raised in order to further minimize the noise occupancy and therefore the readout time (i.e. the width of the current pulses). Administrative procedures have been implemented to avoid the use of the silicon detector in any test that might enhance the probability of running with fixed trigger rates. Finally a trigger inhibit on potential resonant behavior detected with Fast Fourier Transform (FFT) of the silicon readout command has been commissioned and implemented in the DAQ with a minimum impact on the downtime of the experiment.

#### V. CONCLUSIONS

The symptoms of the failures in the SVXII modules were reproduced on spare modules in a controlled environment by emulating the experiment running conditions at the time of the failures. Even if this does not guarantee that the failure mode is the same it is a direct proof that wire-bonds can break according to this mechanism. In the assumption that the mechanism for the failures in the CDF experiment was due to

the resonant vibration excited by Lorentz forces, counter-measures have been applied to minimize the failure rate. No other failures have been detected in  $\sim$ 1 year since their implementation. The failure mode can be prevented in future applications by encapsulating the bonds at their heel.

#### VI. ACKNOWLEDGMENT

The authors would like to thank B. Kephart and M. Tartaglia from the Technical Division at FNAL for the help with the calibration magnet, Greg Selberg from the silicon Detector Facility at FNAL for the optic and mechanics and M. Lindgren and R. Roser for all the support from the CDF Operation Department.

#### VII. REFERENCES

- [1] J. Antos et al., "The SVXII silicon vertex detector upgrade at CDF". Nucl. Instrum. Meth. A383:13-20, 1996.
- [2] G. Bolla "Testing and quality insurance during the construction of the SVXII silicon detector". Nucl. Instrum. Meth., vol. A473, pp. 53-60, 2001.
- [3] M. Garcia-Sciveres et al., "Readout electronics architecture and packaging for the CDF silicon upgrade". Nucl. Instrum. Meth., vol. A392, pp. 375-379, 1997.
- [4] Y. Gotra et al., "The port card for the silicon vertex detector upgrade of the collider detector at Fermilab". IEEE Trans. Nucl. Sci., vol. 48, pp. 504-508, 2001.
- [5] S. Hou, "Experience with the parallel optical link for the CDF silicon detector". Nucl. Instrum. Meth., vol. A511, pp. 166-170, 2003.
- [6] M. Garcia-Sciveres, et al., "The SVX3d integrated circuit for deadtimeless silicon strip readout". Nucl. Instrum. Meth., vol. A435, pp 166-170, 1999.
- [7] T. Zimmerman et al., "SVX3: a dead-timeless readout chip for silicon strip detectors". Nucl. Instrum. Meth., vol. A409, pp 369-374, 1998.
- [8] More details about the FEA analysis can be found at the following URL: [www-cdf.fnal.gov/upgrades/silicon/TASK-Force/FEA.html](http://www-cdf.fnal.gov/upgrades/silicon/TASK-Force/FEA.html).
- [9] More details about the Magnet used for these tests can be found at the following URL: <http://www-cdf.fnal.gov/upgrades/TOF/doc/notes/cdf-2573/node36.html>.
- [10] T. Raymond et al. "Brittle cracks induced in AlSi wire by the ultrasonic bonding tool vibrations". IEEE Transaction on Component, Hybrids and Manufacturing Technology, vol. 14, no. 4, December 1991.